Novel SαS PDF Approximations and Their Applications in Wireless Signal Detection

Yunfei Chen, *Senior Member, IEEE,* Jiming Chen, *Senior Member, IEEE*

***Abstract*— Three new approximations to the probability density function (PDF) of the symmetric alpha stable (SαS) distribution are proposed. The first two approximations use rational functions while the third approximation uses power functions. Using these approximations, new detectors for signals in symmetric alpha stable noise are also derived. Numerical results show that all these new approximations have good accuracies. Numerical results also show that the new detectors based on these approximations outperform the existing detectors, especially when the characteristic exponent of the symmetric alpha stable distribution is small.**

***Index Terms*— Approximation, bit error rate, detection, symmetric alpha stable.**

I. Introduction

Alpha stable distributions have received great research interest in recent years, owing to its accuracy in modeling the heavy-tailed experimental data [1]. For example, it has been reported that the atmospheric noise can be well modeled as alpha stable distributed [1]. In financial application, some stock price was also fit better with the alpha stable model [2]. In wireless communications, the multiple access interference in the presence of a field of Poisson interferers or scatters can also be described as alpha stable distributed [3]. In addition to its experimental value, the alpha stable distributions also have theoretical importance. According to a generalization of the central limit theorem, the sum of independent and identically distributed random variables with infinite variance converges to an alpha stable distribution when the number of random variables is large [4]. This is similar to the Gaussian distribution for the sum of independent and identically distributed random variables with finite variance.

Despite its experimental and theoretical value, a relatively few works have been conducted on the alpha stable model. This is mainly due to the lack of a closed-form expression for the probability density function (PDF) of the alpha stable distribution. In fact, the alpha stable distribution is only defined in terms of its characteristic function [4]. This characteristic function does not have a closed-form expression for the inverse Fourier transform and hence, the PDF of the alpha stable distribution has to be calculated numerically from the characteristic function [5]. This causes great inconvenience in applications related to the alpha stable model. Consequently, simple approximations to the PDF of the alpha stable are preferable for these applications. In [6] and [7], a mixture of Cauchy and Gaussian distributions was used, where [6] provided a simple heuristic formula for the model parameter while [7] required extensive simulation to determine the model parameters. In [8], a mixture of a finite number of Gaussian distributions was used. Unlike that in [6], the approximations in [7] and [8] do not have any numerical way of determining the model parameters and hence extensive simulation is required to calculate these parameters, which is complicated. On the other hand, since the approximation in [6] uses simple formula to calculate the parameters of the mixture, its accuracy can be further improved.

In this paper, three simple parametric approximations to the PDF of the symmetric alpha stable (SαS) distribution are proposed. The first two approximations use rational functions. Nonlinear least squares curve-fitting and point-matching are used to derive the model parameters. The third approximation uses a power function. Nonlinear least squares curve-fitting, point-matching as well as moment-matching are used to obtain its parameters. Numerical results are presented to show and compare the accuracies of these approximations in terms of the Jensen-Shannon divergence. They also show that detectors using new approximations outperform the existing detectors, especially for small characteristic exponent often seen in wireless communications with high path loss exponent.

II. New Approximations

The true PDF of the SαS distribution is given by [9]

$$f_\alpha(x) = \frac{1}{2\pi}\int_{-\infty}^{\infty} e^{-\gamma|\omega|^\alpha + j\delta\omega - j\omega x} d\omega \tag{1}$$

where δ is the location parameter that controls the mode of the PDF, γ is the dispersion parameter that controls the spread of the PDF and α is the characteristic exponent with $0 < \alpha \leq 2$ that controls the shape of the PDF [10]. For simplicity, only the standard alpha stable random variable is considered in the following such that $\delta = 0$ and $\gamma = 1$. For non-standard alpha stable random variables, one can simply replace the argument in the function for the standard alpha stable random variable with its shifted and scaled version. In this case, the true PDF is given by

$$f_\alpha(x) = \frac{1}{2\pi}\int_{-\infty}^{\infty} e^{-|\omega|^\alpha - j\omega x} d\omega. \tag{2}$$

The integration in (2) does not have any closed-form expression, except for $\alpha = 1$ and $\alpha = 2$ which lead to the Cauchy

The authors acknowledge the support of the Open Project Fund (IC14T40), the State Key Laboratory of Industrial Control Technology, Zhejiang University, China.

Yunfei Chen is with the School of Engineering, University of Warwick, Coventry, U.K. CV4 7AL (e-mail: Yunfei.Chen@warwick.ac.uk).

Jiming Chen is with the Department of Control Science and Engineering, Zhejiang University, Hangzhou, Zhejiang, China, 310027. (e-mail: jmchen@ieee.org).

and Gaussian distributions, respectively. Moreover, when α is small, the integration converges very slowly such that it takes a long time to numerically evaluate (2). In [5], transformations to the argument have been done to solve this problem. However, evaluation of the resulting integral is still time-consuming and inconvenient. In [6], a mixture of Cauchy and Gaussian distributions was used to approximate $f_\alpha(x)$ as

$$f_\alpha(x) \approx \frac{\epsilon}{\pi(1+x^2)} + \frac{1-\epsilon}{2\sqrt{\pi}} e^{-\frac{x^2}{4}} \tag{3}$$

where $\epsilon = 2 - \alpha$ is a weighting factor that changes with the value of α. In the following, new approximations to the PDF of the SαS distribution are derived.

A. Approximation Using Rational-based Mixture of Cauchy

The first new approximation is a mixture of two Cauchy distributions given by

$$f_\alpha(x) \approx g_1(x) = \frac{a_1}{1+b_1x^2} + \frac{c_1}{1+d_1x^2}. \tag{4}$$

This is motivated by the following observations.

First, according to [4, Prop. 1.3.1], the SαS random variable can be expressed as $X = Y \cdot Z$, where Y is the ordinary alpha stable random variable totally skewed to the right with PDF $f_Y(y)$ that has the same α as X and Z is the Cauchy random variable with PDF $f_Z(z) = \frac{1}{1+z^2}$, when $\alpha < 1$. Then, the PDF of the SαS random variable X can be calculated as $f_\alpha(x) = \int_{-\infty}^{\infty} \frac{1}{1+(x/y)^2} f_Y(y) \frac{1}{|y|} dy$. This integral can be approximated by a sum such that one has $f_\alpha(x) \approx \sum_{i=1}^{N} \frac{1}{1+(x/y_i)^2} \frac{f_Y(y_i)\Delta y}{|y_i|}$. The more terms used in the approximation, the more accurate but the more complicated the approximation will be. Considering the tradeoff between accuracy and complexity, one can take two terms in the approximation to give (4). Theoretically, this only applies to $\alpha < 1$. However, for engineering use, one could also extend this to $\alpha > 1$, as this is after all an approximation.

Second, in [6] and [7], a mixture of Cauchy and Gaussian distributions was used to approximate the exact PDF of the SαS distribution by controlling the weighting factors for the Cauchy and Gaussian PDFs. The core idea is to obtain different PDFs of the SαS distribution using different weighting factors in the mixture. The same idea can actually be applied to a mixture of two Cauchy distributions by controlling the weighting factors a_1 and c_1 as well as the coefficients of the second-order terms b_1 and d_1, as proposed in (4). This not only gives higher accuracy, especially for small values of α, as will be shown later, but also gives simpler detector structures, as one does not need to calculate the exponential function that is required in [6].

The parameters of a_1, b_1, c_1 and d_1 can be determined in different ways.

1) LS: First, one can use nonlinear least squares (LS) curve-fitting. MATLAB has such a built-in package. Using this package, the values of a_1, b_1, c_1 and d_1 can be calculated as in Table I. In the fitting, the argument is considered from -10 to 10 with a step size of 0.1. The same range and resolution are used for all the other curve-fittings. Note that the choice of this range will affect the approximation accuracy. This is one of the heuristic characteristics of the LS method. For those values that are not listed, similar fitting methods could be used, or one can further fit the parameters as functions of α. It is noted from Table I that the values of parameters for $1 < \alpha < 2$ and for $0 < \alpha < 1$ have different patterns. Thus, these values can be fitted as functions of α for two different intervals as

TABLE I

THE VALUES OF a_1, b_1, c_1 AND d_1 IN $g_1(x)$ FOR DIFFERENT VALUES OF α VIA NONLINEAR LS.

α	a_1	b_1	c_1	d_1
1.9	-6.859	0.1517	7.15	0.1595
1.7	-9.347	0.1924	9.642	0.1988
1.5	-16.88	0.2441	17.18	0.2480
1.3	-181.0	0.3093	181.3	0.3097
1.1	-5.525	0.3830	5.829	0.3957
0.9	0.3027	1.534	0.03155	0.2087
0.7	0.3285	4.465	0.06878	0.2476
0.5	0.4905	31.04	0.1242	0.5962
0.3	2.2371	1037	0.2290	3.1219

$$a_1 = -171.0 \times e^{-\frac{(\alpha-1.307)^2}{0.06478^2}} - 14.71 \times e^{-\frac{(\alpha-1.477)^2}{0.4044^2}} \tag{5a}$$

$$b_1 = 1.455 \times e^{-1.19\alpha} \tag{5b}$$

$$c_1 = -171.1 \times e^{-\frac{(\alpha-1.307)^2}{0.06477^2}} + 14.98 \times e^{-\frac{(\alpha-1.477)^2}{0.4119^2}} \tag{5c}$$

$$d_1 = 1.299 \times e^{-1.104\alpha} \tag{5d}$$

for $1 < \alpha < 2$ and

$$a_1 = 79.95 \times e^{-12.51\alpha} + 0.3998 \times e^{-0.3262\alpha} \tag{6a}$$

$$b_1 = 3.591 \times 10^5 \times e^{-19.59\alpha} + 135.1 \times e^{-5.005\alpha} \tag{6b}$$

$$c_1 = 0.5812 \times e^{-3.104\alpha} \tag{6c}$$

$$d_1 = 53.83 \times e^{-9.642\alpha} + 0.114 \times e^{0.6378\alpha} \tag{6d}$$

for $0 < \alpha < 1$.

Note that this may not be a problem for signal detection, as knowledge of α can be acquired by either direct estimation [10] or indirect calculation from the path loss exponent [3] before detection. In the case when α is not known for signal detection, these formulas cannot be used. Nevertheless, the detector performances will be examined with estimation errors later. For parameter estimation, these formulas cannot be used, as one does not know if α is larger than 1 or smaller than 1. This will be left as a future research topic. The curve-fitting is heuristic and normally depends on the range of α considered. However, in this case, since $0 < \alpha \leq 2$ is a very limited range, it works well.

2) PMM: The second method of determining these parameters is obtained by using point-matching method (PMM). Essentially, four values of the true PDF and the four corresponding values of $g_1(x)$ are calculated and then four equations can be established by equating them to find the four unknown parameters. Specifically, using $f_\alpha(0)$, $\int_{-\infty}^{\infty} f_\alpha(x)dx$, $\int_{-\infty}^{\infty} f_\alpha^2(x)dx$ and the p-th order moment, one has

$$a_1 + c_1 = \frac{1}{\pi\alpha}\Gamma\left(\frac{1}{\alpha}\right) \tag{7a}$$

$$\frac{\pi a_1}{\sqrt{b_1}} + \frac{\pi c_1}{\sqrt{d_1}} = 1 \tag{7b}$$

$$\frac{\pi a_1^2}{2\sqrt{b_1}} + \frac{\pi c_1^2}{2\sqrt{d_1}} + \frac{2\pi a_1 c_1}{\sqrt{d_1}+\sqrt{b_1}} = \frac{2^{-\frac{1}{\alpha}}}{\alpha\pi}\Gamma\left(\frac{1}{\alpha}\right) \tag{7c}$$

$$\left(\frac{a_1}{b_1^{\frac{p+1}{2}}} + \frac{c_1}{d_1^{\frac{p+1}{2}}}\right)\cdot B\left(\frac{p+1}{2}, \frac{1-p}{2}\right) = \frac{2^{p+1}\Gamma(\frac{p+1}{2})\Gamma(-\frac{p}{\alpha})}{\alpha\sqrt{\pi}\Gamma(-\frac{p}{2})} \tag{7d}$$

where $-1 < p < \alpha$ [11], $\Gamma(\cdot)$ is the Gamma function [12, eq. (8.310.1)], and $B(\cdot,\cdot)$ is the incomplete Beta function [12, eq. (8.380.1)]. The derivations of these equations are given in Appendix A. Using (7a) and (7b), the values of a_1 and c_1 can be expressed as functions of b_1 and d_1. Using these expressions in (7c) and (7d), two equations for b_1 and d_1 can be derived. Then, a two-dimensional search is performed to find the values of b_1 and d_1. Using them in (7a) and (7b), the values of a_1 and c_1 can then be derived.

B. Approximation Using Rational-based Partial Fraction

From (4), a very straightforward extension is to combine the two terms in (4) using partial fraction such that one has

$$f_\alpha(x) \approx g_2(x) = \frac{a_2 + b_2 x^2}{1 + c_2 x^2 + d_2 x^4}. \tag{8}$$

This approximation is similar to (4), but is not equivalent to (4), as the denominator in (8) may not be decomposed to give (4). In other words, (8) is more general than (4), and this generality can give extra accuracy that is not offered by (4), as will be discussed in Section IV. On the other hand, this approximation is more complicated than (4) due to the fourth-order term in the denominator.

1) LS: Using LS, the values of a_2, b_2, c_2 and d_2 can be calculated as in Table II. These values can be fitted as functions of α as

$$a_2 = 0.0303 \times \alpha^{-3.526} + 0.283 \tag{9a}$$

$$b_2 = 0.01047 \times \alpha^{-8.601} + 0.05204 \tag{9b}$$

$$c_2 = 0.1983 \times \alpha^{-7.304} + 0.8007 \tag{9c}$$

$$d_2 = 0.009657 \times \alpha^{-10.86} + 0.2337. \tag{9d}$$

In this case, one has the same functions for all values of α.

2) PMM: Also, using PMM, one has

$$\frac{2^{p+1}\Gamma\left(\frac{p+1}{2}\right)\Gamma\left(-\frac{p}{\alpha}\right)}{\alpha\sqrt{\pi}\Gamma\left(-\frac{p}{2}\right)} = \frac{\frac{\sqrt{2}a_2\Gamma\left(\frac{3}{2}\right)P_{-\frac{p}{2}}^{-\frac{1}{2}}\left(\frac{c_2}{2\sqrt{d_2}}\right)}{\left(\frac{c_2^2}{4d_2}-1\right)^{\frac{1}{4}}B^{-1}\left(\frac{3-p}{2},\frac{p+1}{2}\right)} + \frac{b_2}{\sqrt{d_2}}\frac{\sqrt{2}\Gamma\left(\frac{3}{2}\right)P_{-\frac{p+1}{2}}^{-\frac{1}{2}}\left(\frac{c_2}{2\sqrt{d_2}}\right)}{\left(\frac{c_2^2}{4d_2}-1\right)^{\frac{1}{4}}B^{-1}\left(\frac{1-p}{2},\frac{p+3}{2}\right)}}{\left[\frac{\sqrt{2}a_2\Gamma\left(\frac{3}{2}\right)P_0^{-\frac{1}{2}}\left(\frac{c_2}{2\sqrt{d_2}}\right)}{\left(\frac{c_2^2}{4d_2}-1\right)^{\frac{1}{4}}B^{-1}\left(\frac{3}{2},\frac{1}{2}\right)} + \frac{b_2}{\sqrt{d_2}}\frac{\sqrt{2}\Gamma\left(\frac{3}{2}\right)P_{-1}^{-\frac{1}{2}}\left(\frac{c_2}{2\sqrt{d_2}}\right)}{\left(\frac{c_2^2}{4d_2}-1\right)^{\frac{1}{4}}B^{-1}\left(\frac{1}{2},\frac{3}{2}\right)}\right]^{p+1}} \tag{10}$$

and

$$u\left(\frac{b_2}{\sqrt{d_2}}\right)^2 + v\frac{b_2}{\sqrt{d_2}} + w = 0 \tag{11}$$

TABLE II
THE VALUES OF a_2, b_2, c_2 AND d_2 IN $g_2(x)$ FOR DIFFERENT VALUES OF α VIA NONLINEAR LS.

α	a_2	b_2	c_2	d_2
1.9	0.2802	-0.008263	0.1927	0.0471
1.7	0.2826	-0.003591	0.2593	0.05609
1.5	0.2867	0.003727	0.3636	0.07069
1.3	0.2939	0.01666	0.5427	0.09771
1.1	0.3078	0.03413	0.8838	0.1187
0.9	0.3438	0.1159	1.828	0.3294
0.7	0.3973	0.3876	4.709	1.102
0.5	0.6142	4.075	31.35	18.07
0.3	1.847	43.07	396.3	323.0

for $c_2^2 \geq 4d_2$, where u, v and w are given by (47) in Appendix B.

For $c_2^2 < 4d_2$, one has

$$\frac{2^{p+1}\Gamma\left(\frac{p+1}{2}\right)\Gamma\left(-\frac{p}{\alpha}\right)}{\alpha\sqrt{\pi}\Gamma\left(-\frac{p}{2}\right)} = \frac{\frac{\sqrt{2}a_2\Gamma\left(\frac{3}{2}\right)tP_{\frac{p-2}{2}}^{-\frac{1}{2}}\left(\frac{c_2}{2\sqrt{d_2}}\right)}{\left(1-\frac{c_2^2}{4d_2}\right)^{\frac{1}{4}}B^{-1}\left(\frac{p+1}{2},\frac{3-p}{2}\right)} + \frac{b_2}{\sqrt{d_2}}\frac{\sqrt{2}\Gamma\left(\frac{3}{2}\right)tP_{\frac{p}{2}}^{-\frac{1}{2}}\left(\frac{c_2}{2\sqrt{d_2}}\right)}{\left(1-\frac{c_2^2}{4d_2}\right)^{\frac{1}{4}}B^{-1}\left(\frac{p+3}{2},\frac{1-p}{2}\right)}}{\left[\frac{\sqrt{2}a_2\Gamma\left(\frac{3}{2}\right)tP_{-1}^{-\frac{1}{2}}\left(\frac{c_2}{2\sqrt{d_2}}\right)}{\left(1-\frac{c_2^2}{4d_2}\right)^{\frac{1}{4}}B^{-1}\left(\frac{3}{2},\frac{1}{2}\right)} + \frac{b_2}{\sqrt{d_2}}\frac{\sqrt{2}\Gamma\left(\frac{3}{2}\right)P_0^{-\frac{1}{2}}\left(\frac{c_2}{2\sqrt{d_2}}\right)}{\left(1-\frac{c_2^2}{4d_2}\right)^{\frac{1}{4}}B^{-1}\left(\frac{1}{2},\frac{3}{2}\right)}\right]^{p+1}} \tag{12}$$

and

$$u'\left(\frac{b_2}{\sqrt{d_2}}\right)^2 + v'\frac{b_2}{\sqrt{d_2}} + w' = 0 \tag{13}$$

where $t = \arccos\left(\frac{c_2}{2\sqrt{d_2}}\right)$, u', v' and w' are given by (48) in Appendix B. Equations (10) and (11) or (12) and (13) can be used to find the values of $\frac{c_2}{2\sqrt{d_2}}$ and $\frac{b_2}{\sqrt{d_2}}$. In this case, two one-dimensional searches are required for $\frac{c_2}{2\sqrt{d_2}}$ and $\frac{b_2}{\sqrt{d_2}}$. The value of d_2 can be found by using (40) or (41). Then, b_2 and c_2 can be calculated. Their derivations are given in Appendix B.

C. Power-based Approximations

In this subsection, another new approximation is proposed that uses power functions. It is proposed that the true PDF of the SαS distribution can be approximated as

$$f_\alpha(x) \approx g_3(x) = \frac{a_3}{1 + b_3|x|^{\alpha+1}}. \tag{14}$$

This approximation is motivated by the fact that the true PDF of the SαS distribution decays at a rate of $\frac{1}{x^{\alpha+1}}$ at the tails [9].

1) LS: Using LS, one has the values of a_3 and b_3 as in Table III. The values in Table III can then be fitted as functions of α as

$$a_3 = 5.633 \times e^{-6.131\alpha} + 0.3447 \times e^{-0.1197\alpha} \tag{15a}$$

$$b_3 = 497.2 \times e^{-9.9445\alpha} + 5.067 \times e^{-1.629\alpha}. \tag{15b}$$

The fitting functions in (5), (6), (9) and (15) are chosen as the best fits after testing all commonly used nonlinear functions, including Gaussian, exponential, rational, polynomial

TABLE III
THE VALUES OF a_3 AND b_3 IN $g_3(x)$ FOR DIFFERENT VALUES OF α VIA NONLINEAR LS.

α	a_3	b_3
1.9	0.2781	0.2691
1.7	0.2815	0.3401
1.5	0.2864	0.4388
1.3	0.2942	0.5841
1.1	0.3069	0.8051
0.9	0.3426	1.313
0.7	0.3934	2.318
0.5	0.5895	6.672
0.3	2.945	95.62

and power functions, based on the observations from their plots with respect to α. This shows another heuristic aspect of curve-fitting.

2) PMM: Also, using PMM, one has

$$a_3 = \frac{1}{\pi\alpha}\Gamma\left(\frac{1}{\alpha}\right) \tag{16a}$$

$$\frac{2a_3}{(\alpha+1)b_3^{\frac{1}{\alpha+1}}} B\left(\frac{1}{\alpha+1}, \frac{\alpha}{\alpha+1}\right) = 1 \tag{16b}$$

$$\frac{2a_3^2}{b_3^{\frac{1}{\alpha+1}}} \frac{\alpha\pi}{(\alpha+1)^2} \csc\left(\frac{\pi\alpha}{\alpha+1}\right) = \frac{2^{-\frac{1}{\alpha}}\Gamma(\frac{1}{\alpha})}{\pi\alpha} \tag{16c}$$

$$\frac{a_3}{b_3} = \frac{\alpha}{\pi}\Gamma(\alpha)\sin\left(\frac{\alpha\pi}{2}\right). \tag{16d}$$

In this case, there are four equations available but one only needs to find the values of two unknown parameters a_3 and b_3. Thus, there are six different solutions. Using (16a) and (16b), one has

$$a_3 = \frac{\Gamma(\frac{1}{\alpha})}{\pi\alpha} \tag{17a}$$

$$b_3 = \left[\frac{2\Gamma(\frac{1}{\alpha})}{\alpha(\alpha+1)} \csc\left(\frac{\pi}{\alpha+1}\right)\right]^{\alpha+1}. \tag{17b}$$

Using (16a) and (16c), one has

$$a_3 = \frac{\Gamma(\frac{1}{\alpha})}{\pi\alpha} \tag{18a}$$

$$b_3 = \left[\frac{2^{1+\frac{1}{\alpha}}\Gamma(\frac{1}{\alpha})}{(\alpha+1)^2} \csc\left(\frac{\alpha\pi}{\alpha+1}\right)\right]^{\alpha+1}. \tag{18b}$$

Using (16b) and (16c), one has

$$a_3 = \frac{2^{-\frac{1}{\alpha}}\Gamma(\frac{1}{\alpha})(\alpha+1)}{\pi\alpha^2} \cdot \frac{\csc(\frac{\pi}{\alpha+1})}{\csc(\frac{\alpha\pi}{\alpha+1})} \tag{19a}$$

$$b_3 = \left[\frac{2^{1-\frac{1}{\alpha}}\Gamma(\frac{1}{\alpha})}{\alpha^2} \cdot \frac{\csc^2(\frac{\pi}{\alpha+1})}{\csc(\frac{\alpha}{\alpha+1}\pi)}\right]^{\alpha+1}. \tag{19b}$$

Using (16a) and (16d), one has

$$a_3 = \frac{\Gamma(\frac{1}{\alpha})}{\pi\alpha} \tag{20a}$$

$$b_3 = \frac{\Gamma(\frac{1}{\alpha})}{\alpha^2\Gamma(\alpha)\sin(\frac{\alpha\pi}{2})}. \tag{20b}$$

Using (16b) and (16d), one has

$$a_3 = \left[\frac{(\alpha+1)}{2\alpha\Gamma(\alpha)\sin(\frac{\alpha\pi}{2})\csc(\frac{\pi}{(\alpha+1)})}\right]^{\frac{\alpha+1}{\alpha}} \cdot \frac{\Gamma(\alpha)\alpha}{\pi} \cdot \sin(\frac{\alpha\pi}{2}) \tag{21a}$$

$$b_3 = \left[\frac{(\alpha+1)}{2\alpha\Gamma(\alpha)\sin(\frac{\alpha\pi}{2})\csc(\frac{\pi}{(\alpha+1)})}\right]^{\frac{\alpha+1}{\alpha}}. \tag{21b}$$

Using (16c) and (16d), one has

$$a_3 = \left[\frac{2^{-\frac{1}{\alpha}}(\alpha+1)^2}{2\alpha^4\Gamma(\alpha)(\sin(\frac{\alpha\times\pi}{2}))^2\csc(\frac{\alpha\times\pi}{(\alpha+1)})}\right]^{\frac{\alpha+1}{2\alpha+1}} \cdot \frac{\Gamma(\alpha)\alpha}{\pi} \cdot \sin(\frac{\alpha\pi}{2}) \tag{22a}$$

$$b_3 = \left[\frac{2^{-\frac{1}{\alpha}}(\alpha+1)^2}{2\alpha^4\Gamma(\alpha)(\sin(\frac{\alpha\times\pi}{2}))^2\csc(\frac{\alpha\times\pi}{(\alpha+1)})}\right]^{\frac{\alpha+1}{2\alpha+1}}. \tag{22b}$$

3) MMM: The p-th order moment can also be derived as

$$\frac{2a_3}{b_3^{\frac{p+1}{\alpha+1}}} \cdot \frac{\pi}{\alpha+1} \cdot \csc\left(\frac{p+1}{\alpha+1}\pi\right) = \frac{2^{p+1}\Gamma(\frac{p+1}{2})\Gamma(-\frac{p}{\alpha})}{\alpha\sqrt{\pi}\Gamma(-\frac{p}{2})} \tag{23}$$

where $-1 < p < \alpha$. Using moment-matching method (MMM) by choosing any two orders of moments p_1 and p_2, one has

$$a_3 = \frac{2^{p_1}\Gamma(\frac{p_1+1}{2})\Gamma(-\frac{p_1}{\alpha})(\alpha+1)}{\alpha\sqrt{\pi}\pi\Gamma(-\frac{p_1}{2})\csc(\frac{p_2+1}{\alpha+1}\pi)} \cdot \left[2^{p_1-p_2}\frac{\Gamma(\frac{p_1+1}{2})\Gamma(-\frac{p_1}{\alpha})\Gamma(-\frac{p_2}{2})\csc(\frac{(p_2+1)\pi}{\alpha+1})}{\Gamma(\frac{p_2+1}{2})\Gamma(-\frac{p_2}{\alpha})\Gamma(-\frac{p_1}{2})\csc(\frac{(p_1+1)\pi}{\alpha+1})}\right]^{\frac{p_1+1}{p_2-p_1}} \tag{24a}$$

$$b_3 = \left[2^{p_1-p_2}\frac{\Gamma(\frac{p_1+1}{2})\Gamma(-\frac{p_1}{\alpha})\Gamma(-\frac{p_2}{2})\csc(\frac{(p_2+1)\pi}{\alpha+1})}{\Gamma(\frac{p_2+1}{2})\Gamma(-\frac{p_2}{\alpha})\Gamma(-\frac{p_1}{2})\csc(\frac{(p_1+1)\pi}{\alpha+1})}\right]^{\frac{\alpha+1}{p_2-p_1}}. \tag{24b}$$

The derivations of these equations are given in Appendix C.

In Tables I, II and III, only the values from LS are shown, because these values are used to find the analytical relationships between α and the model parameters in (5), (6), (9) and (15). Values from other methods are not shown in the tables for this purpose due to the fact that they have already had these analytical relationships and also due to the limited space.

D. Further Notes

Note that PMM and MMM provide simple closed-form expressions for the power-based approximation. Thus, they are particularly useful for the power-based approximation. For the rational-based approximations using PMM, grid searches have to be performed. The search time can be saved by using the results from the LS method as the starting points and by performing selective searches for the range. For example, depending on the LS result, the first search can be from 0 to 10000 with a step size of 1000 to determine the first valid digit. The second search is based on the first search. If the first search gives 2000 as the best value, the second search will be from 1000 to 3000 with a step size of 100 to determine the second valid digit, and so on until the third digit after the decimal point is determined. Then, the selective search is

over. Note also that reference [6] has much lower complexity in the calculation of the parameters than the approximations proposed in this paper, as it only needs to determine the value of ϵ which is a very simple function of α. This simplicity comes at the cost of accuracy loss in certain cases.

Note that the above approximations are not normalized, except those based on PMM that uses $\int_{-\infty}^{\infty} f_\alpha(x)dx$. This does not affect signal detection, as the normalization factor will be canceled out in the likelihood ratio. On the other hand, the approximations based on LS, MMM and PMM that does not use $\int_{-\infty}^{\infty} f_\alpha(x)dx$ can be normalized by dividing the approximations with the left sides of the equations in (7b), (40), (41) and (16b). Denote the normalized approximations as $h_1(x)$, $h_2(x)$ and $h_3(x)$ for $g_1(x)$, $g_2(x)$ and $g_3(x)$, respectively.

III. Detectors based on new approximations

In this section, detectors based on the new approximations derived in the previous section will be obtained. These detectors are based on the maximum likelihood (ML) detection principle but use the new approximations to replace the true PDF of the SαS distribution instead. Specifically, consider a binary phase shift keying (BPSK) signal with equal *a priori* probabilities. The i-th received signal sample can be expressed as

$$x_i = A * s + I_i \tag{25}$$

where A is the channel gain, s is the BPSK signal and I_i is the SαS interference or noise sample. Thus, one has the likelihood ratio as $\frac{\prod_{i=1}^{N} f_{x_i}(x|s=1)}{\prod_{i=1}^{N} f_{x_i}(x|s=-1)}$ and the log-likelihood ratio as $\Psi = \log\{\frac{\prod_{i=1}^{N} f_{x_i}(x|s=1)}{\prod_{i=1}^{N} f_{x_i}(x|s=-1)}\}$, where $f_{x_i}(x|s=1) = f_{I_i}(x-A)$ and $f_{x_i}(x|s=-1) = f_{I_i}(x+A)$. Assuming that $s=1$ and $s=-1$ have equal *a priori* probabilities, the detection threshold becomes $\log\{\frac{Pr\{s=-1\}}{Pr\{s=1\}}\} = 0$. Then, using the ML principle, the detector becomes $\Psi > 0$ for $s=1$ and $\Psi < 0$ for $s=-1$. Using (4), (8), (14), the decision variables are

$$\Psi_1 = \sum_{i=1}^{N} \log\left\{\frac{\frac{a_1}{(1+b_1(x_i-A)^2)} + \frac{c_1}{(1+d_1(x_i-A)^2)}}{\frac{a_1}{(1+b_1(x_i+A)^2)} + \frac{c_1}{(1+d_1(x_i+A)^2)}}\right\} \tag{26}$$

$$\Psi_2 = \sum_{i=1}^{N} \log\left\{\frac{(1+c_2(x_i+A)^2+d_2(x_i+A)^4)}{(1+c_2(x_i-A)^2+d_2(x_i-A)^4)} \cdot \frac{(a_2+b_2(x_i-A)^2)}{(a_2+b_2(x_i+A)^2)}\right\} \tag{27}$$

and

$$\Psi_3 = \sum_{i=1}^{N} \log\left\{\frac{1+b_3|x_i+A|^{\alpha+1}}{1+b_3|x_i-A|^{\alpha+1}}\right\} \tag{28}$$

respectively, where N is the number of samples for each bit or symbol. It was reported in the literature that the Cauchy detector and the Myriad detector have good performances with simple structures, similar to the proposed detectors here. The Cauchy detector is given by [9, eq. (3-18)]

$$\Psi_4 = \sum_{i=1}^{N} \log\left\{\frac{1+(x_i+A)^2}{1+(x_i-A)^2}\right\} \tag{29}$$

while the Myriad detector is given by

$$\Psi_5 = \sum_{i=1}^{N} \log\left\{\frac{k^2+(x_i+A)^2}{k^2+(x_i-A)^2}\right\} \tag{30}$$

where $k = \sqrt{\frac{\alpha}{2-\alpha}}$ is a simple empirical form by taking three points of optimality associated with the Myriad and is found to be consistently efficient in many cases examined in [13], [14]. The exact optimal k depends on the cost function and often does not have a simple closed-form expression [13], [14] and therefore, is not compared here. In the case when $\gamma \neq 1$, one can replace $x_i - A$ and $x_i + A$ with $\frac{x_i-A}{\gamma^{1/\alpha}}$ and $\frac{x_i+A}{\gamma^{1/\alpha}}$, respectively, as the above detectors are based on the standard PDF in (2) that can be obtained from the general PDF in (1) by letting $\omega' = \omega\gamma^{1/\alpha}$ and then $x' = \frac{x-\delta}{\gamma^{1/\alpha}}$. This can be verified by using the general PDF in the ML detector and then replacing it using the shifted and scaled version of the standard PDF.

IV. Numerical Results and Discussion

In this section, the accuracies of the proposed approximations will be examined. Also, the detectors based on these approximations will be compared in terms of bit error rate (BER). The BER will be simulated for BPSK signals with respect to the geometric signal-to-noise ratio (SNR) defined as $\Omega = \frac{A^2 N}{2\gamma^{2/\alpha} C_g^{\frac{2}{\alpha}-1}}$ [17], where $C_g = 1.78$. The geometric power of a random variable is defined as $e^{E\{\log\{X\}\}}$, where $E\{\cdot\}$ is the expectation and X is the interested random variable. The traditional power $E\{X^2\}$ does not exist for random variables with infinite variance, such as SαS, and the geometric power is reported to be a good alternative in this case [17]. In the simulation, $N = 10$, a number of 10^6 trials, $\alpha = 1.8$, $\alpha = 0.5$ and $\alpha = 0.3$ are used. Also, imperfect estimate of α is assumed as Gaussian with mean α and variance $\epsilon = 0.002$, unless stated otherwise. This is based on the sample characteristic function estimator for α that can achieve a mean squared error (MSE) of less than 0.002 with enough samples [18].

Table IV shows the Jensen-Shannon divergence (JSD) of different approximations with different methods. JSD is a symmetric version of the commonly used Kullback-Leibler divergence. Since the JSD is only represented in an integral form and does not have a closed-form expression for SαS, it is calculated using the Simpson's rule between -1000 and 1000 with a step size of 0.1. Since $\alpha > 0$ and $-1 < p < \alpha$, the order of moment is chosen between -1 and 0 for small values of α such that it always exists. For PMM of $g_1(x)$, $p = -0.9$, $p = -0.7$, $p = -0.5$, $p = -0.3$ and $p = -0.1$ with a step size of 0.2 are tested to cover the chosen range, and the smallest JSD is given in Table IV. For PMM of $g_2(x)$, $p = -0.9$, $p = -0.7$, $p = -0.5$ and $p = -0.3$ are tested with a step size of 0.2 to cover the chosen range. For PMM of $g_3(x)$, all six possible solutions are tested. It is found that (18) gives the smallest JSD, given in Table IV. For MMM of $g_3(x)$, $p_1 = -0.9$, $p_2 = 0.1$, $p_1 = -0.7$, $p_2 = -0.1$, $p_1 = -0.5$, $p_2 = -0.3$ are tested for $\alpha = 0.3$, $p_1 = -0.9$, $p_2 = 0.3$, $p_1 = -0.7$, $p_2 = -0.1$, $p_1 = -0.5$, $p_2 = -0.1$ are tested for $\alpha = 0.5$, $p_1 = -0.9$, $p_2 = 1.7$, $p_1 = -0.7$, $p_2 = 1.5$,

TABLE IV
THE JSD OF DIFFERENT APPROXIMATIONS WITH DIFFERENT METHODS OF PARAMETER CALCULATIONS.

Method	$\alpha = 1.8$	$\alpha = 0.5$	$\alpha = 0.3$
$h_1(x)$, LS	0.01643	0.03105	0.08311
$h_1(x)$, PMM	0.01415	0.02116	0.05857
$h_2(x)$, LS	0.008399	0.03088	0.1270
$h_2(x)$, PMM	0.03124	0.02341	0.07229
$h_3(x)$, LS	0.01020	0.009127	0.02903
$h_3(x)$, PMM	0.008542	0.01280	0.07459
$h_3(x)$, MMM	0.008716	0.004903	0.01419
[6]	0.001982	0.02586	0.1365

$p_1 = -0.5$, $p_2 = 1.3$, $p_1 = -0.3$, $p_2 = 1.1$, $p_1 = -0.3$, $p_2 = 1.1$, $p_1 = 0.1$, $p_2 = 0.7$ are tested for $\alpha = 1.8$, with decreasing distances between p_1 and p_2, and the smallest JSD is given in Table IV. Note that other values of p and other combinations of multiple orders can also be tested. Due to the limited space and the similar method used, they are not given here to make the paper compact.

Several important observations can be made from Table IV. First, comparing the new approximations with [6], one sees that the new approximations have smaller JSD than [6] for most cases of $\alpha = 0.3$ and $\alpha = 0.5$, and larger JSD for $\alpha = 1.8$. This is because when α increases, the decaying rate of the tails increases (exponential rate in the limiting case when $\alpha = 2$) to a degree that it cannot be captured well by the new approximations, as the maximum decaying rate for $h_1(x)$ and $h_2(x)$ is $\frac{1}{x^2}$, and for $h_3(x)$ is $\frac{1}{x^{\alpha+1}}$, smaller than the exponential rate offered by the Gaussian term in [6], which weighs more as α increases. Second, among the new approximations, $h_3(x)$ has the lowest overall JSD, followed by $h_1(x)$ and then by $h_2(x)$. For $\alpha = 1.8$, $h_2(x)$ using LS has a JSD of 0.008399, only about half of $h_1(x)$ using LS. This verifies the necessity of using $g_2(x)$ in (8), in addition to $g_1(x)$ in (4). It can be shown that, when $\alpha = 1.8$, $c_2^2 - 4d_2 < 0$ such that the denominator of $g_2(x)$ in (8) cannot be decomposed into the product of two terms. As a result, $g_2(x)$ in (8) is not equivalent to $g_1(x)$ in (4). Thus, the generality of $g_2(x)$ in (8) does offer extra accuracy in this case. Third, comparing different parameter calculation methods for each approximation, one sees that PMM gives the smallest JSD for $h_1(x)$ and $h_2(x)$ in most cases, while MMM gives the smallest JSD for $h_3(x)$. Finally, the value of JSD increases when the value of α decreases in most cases. This is because the true PDF of the SαS distribution becomes more impulsive when α decreases and hence, approximations become more difficult to track this dramatic change.

Fig. 1 compares the approximate PDFs using the LS method and the exact PDF graphically. Only the positive part is shown as the PDF is symmetric around 0. As expected, $h_3(x)$ has the same decaying rate as the exact PDF, as it is designed based on this observation. For $h_1(x)$, $h_2(x)$ and [6], they have similar decaying rates, all of which are faster than that of the exact PDF, as expected, as the exact PDF decays at $\frac{1}{x^{1.5}}$ for $\alpha = 0.5$ at $\frac{1}{x^{1.3}}$ for $\alpha = 0.3$ while $h_1(x)$, $h_2(x)$ and [6] decay at $\frac{1}{x^2}$ (the Gaussian term in [6] can be ignored for $x > 10$ from the figures.). However, [6] varies a lot when approaching the tail due to the interaction between the Cauchy term and the Gaussian term in the mixture that have different decaying rates, while $h_1(x)$, $h_2(x)$ are quite consistent. In summary, the new approximations seem to track the exact PDF better than the existing approximation in [6] in Fig. 1.

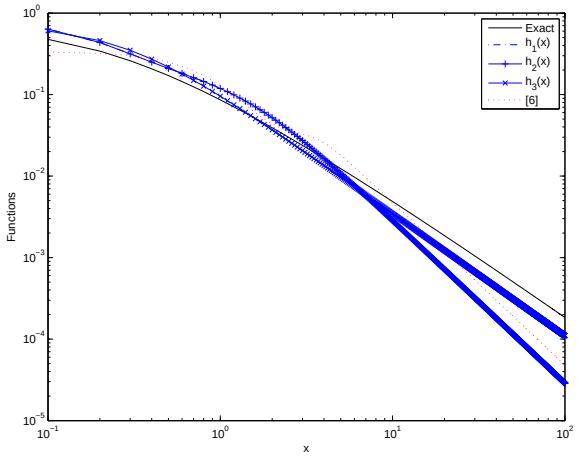

Fig. 1. Comparison of the positive tails of different approximations when $\alpha = 0.5$ and $\gamma = 1$.

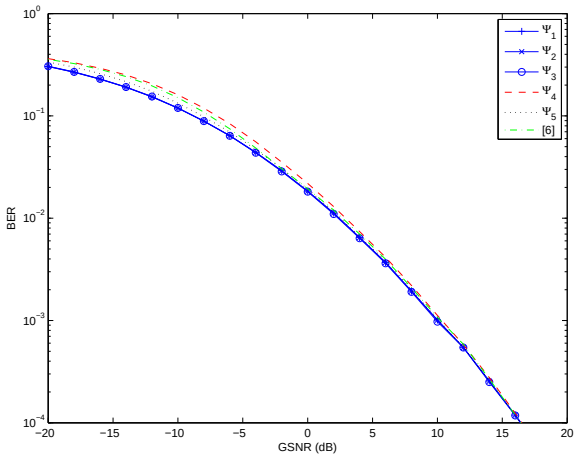

Fig. 2. BER vs. GSNR for different detectors when $\alpha = 0.5$ and $\gamma = 1$.

Figs. 2 - 4 show the BER performances of different detectors under different conditions when $\gamma = 1$. In these figures, only LS is used for the new approximations for better readability. Fig. 2 shows the detector performances for $\alpha = 0.5$. In this case, the detector performances have significant differences. Specifically, Ψ_1, Ψ_2 and Ψ_3 have the best performances and their performances are indistinguishable from each other. The Myriad detector Ψ_5 has the second best overall performance, while Cauchy Ψ_4 and [6] have the worst overall performances. The performance gains decrease when the SNR increases. The reason why the performances of all the detectors converge at smaller BER is that the SαS noise is less important in signal detection for larger values of SNR (smaller BER) where signals dominate such that the approximation error does not determine the BER performance in this case.

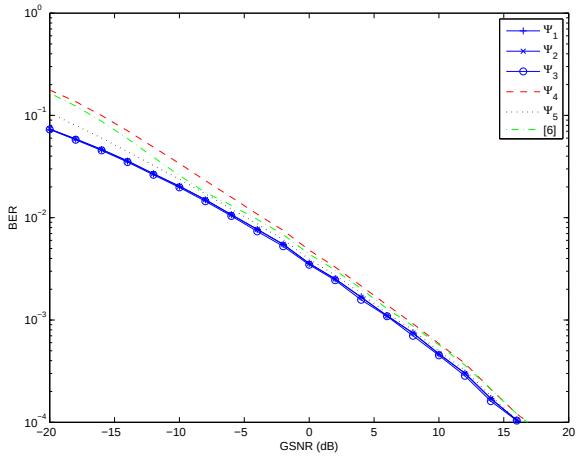

Fig. 3. BER vs. GSNR for different detectors when $\alpha = 0.3$ and $\gamma = 1$.

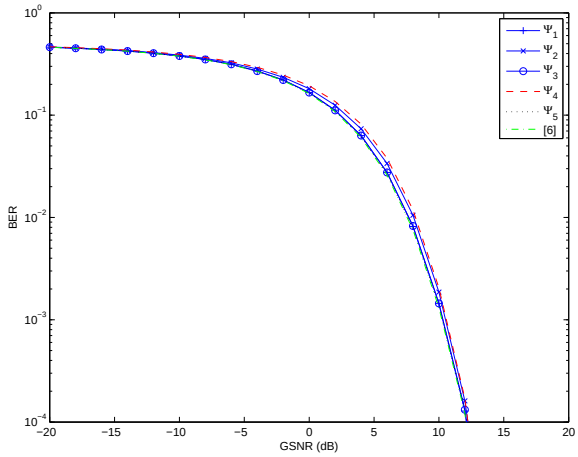

Fig. 4. BER vs. GSNR for different detectors when $\alpha = 1.8$ and $\gamma = 1$.

Fig. 3 shows the BER performances of the detectors for $\alpha = 0.3$. In this case, the performance gains of the new detectors are larger than those in Fig. 2. For example, at a BER of 0.08, the performance gain over Myriad is about 2 dB, and the performance gain over Cauchy and [6] is about 6 dB. Importantly, the performance gain is larger at smaller values of SNR, when it is needed most. Although a BER value of 0.1 or 0.01 and a SNR value of -20 dB are not common for data-oriented or cellular communications systems, it is quite common in optical wireless communications systems [19] that may suffer from atmospheric turbulence often modeled as alpha stable distributed [1], in air-borne wireless sensor networks with very weak transmitted signals but large node density, or in radar communications, such as passive or long-range radars, where SNR is often small as the signal from the target is weak. For example, in distributed sensor networks, the effective BER could reach 0.1 or 0.2 for various signal processing algorithms [20]. In ultra-wideband radars [21], the SNR could be as low as -56 dB or -86 dB, and in some sensor applications [22], the SNR could be at -6 dBm or -36 dB.

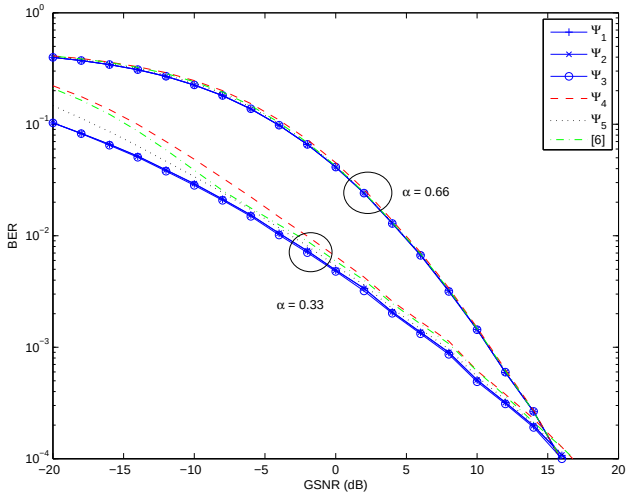

Fig. 5. BER vs. GSNR for different detectors when $\gamma = 1$ and values of α are not listed in the tables.

The performance gains of the new detectors are in the range between 2 dB and 6 dB near the SNR value of -20 dB. These are significant in this operating region [23], [24].

Fig. 4 shows the detector performances for $\alpha = 1.8$. In this case, the Cauchy detector has the worst performance, while all the other detectors have similar performances. It can be seen that [6] has a slightly better performance than all other detectors, as expected, as none of the other detectors can capture the exponentially decaying rate of the SαS tails better than [6] when α is large, inlcuding the Myriad detector.

From Figs. 2 - 4, the new detectors outperform the existing detectors in most cases, and the performance gain increases when α decreases, implying that these new detectors are more suitable for impulsive noise. In wireless communications with a Poisson field of scatters, α is often determined by $\alpha = \frac{2}{\beta}$ for a plane [3, eq. (16)] and $\alpha = \frac{3}{\beta}$ for a volume [3, eq. (17)], where β is the path loss exponent in the channel. On the other hand, it was reported in [25, Table 4.2] that the path loss exponent β is often between 2 and 6 for different application scenarios. Using these two results, the value of α can be calculated as between 1 and 0.33 if a plane is considered. For future wireless systems with higher carrier frequency, such as the proposed 5G system at 26 GHz, β will be larger due to higher attentuation, leading to even smaller α. This observation is not confirmed by any experimental measurements and does not exclude other applications with α larger than 1 either. Rather, it comes directly from combining results in [3] and [25].

Fig. 5 shows the performances of the detectors for values of α that are not listed in the tables. Similar observations to those from Figs. 2 - 4 can be made. This verifies the usefulness of the derived analytical expressions for the LS method. From Figs. 2 - 4, one can see that the proposed new approximations offer performance gains in detection mainly for values of $\alpha \leq 0.5$ in the cases examined. This gain is very small when $\alpha > 0.5$, as can be seen from Fig. 5 when $\alpha = 0.66$. This

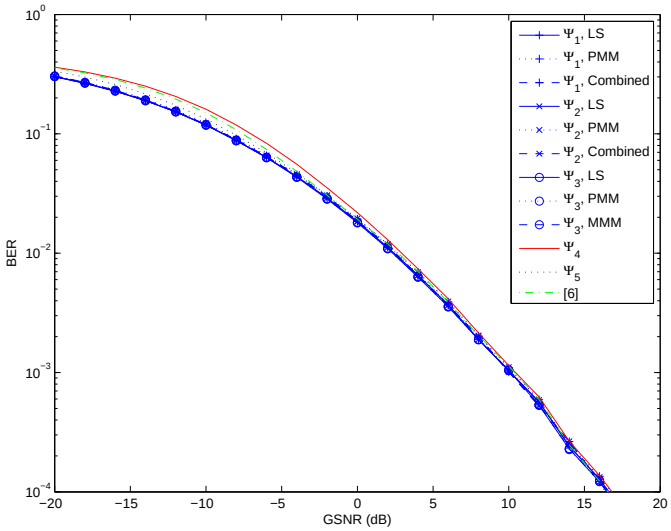

Fig. 6. BER vs. GSNR for different detectors when $\alpha = 0.5$ and $\gamma = 1$ using different proposed methods.

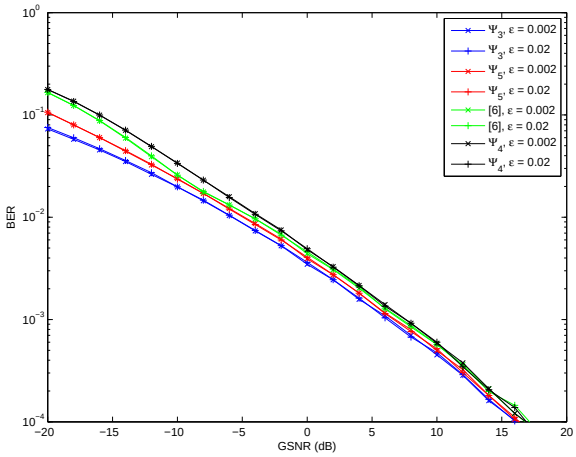

Fig. 7. BER vs. GSNR for Ψ_3, Ψ_4, Ψ_5 and [6] when $\alpha = 0.3$ and $\gamma = 1$.

agrees with the previous conclusion that the new detectors are more suitable for impulsive noise with large path loss. Fig. 6 shows the performances of the detectors where different proposed methods are used to calculate the approximation parameters. One sees that the difference between different methods of the proposed detectors is trivial compared with the difference between the proposed detectors and the existing detectors. Our numerical tests show that the PMM method, although with higher complexity due to the grid search, offers little gain in detection performance over the LS method in the cases examined. Thus, for signal detection, the LS method is a better choice. For other applications that require a more accurate approximation, the PMM method may be a better choice according to Table IV.

Fig. 7 examines the sensitivities of the detectors to the errors in the estimation of α. One sees that in general the detectors are not sensitive to the estimation error when the

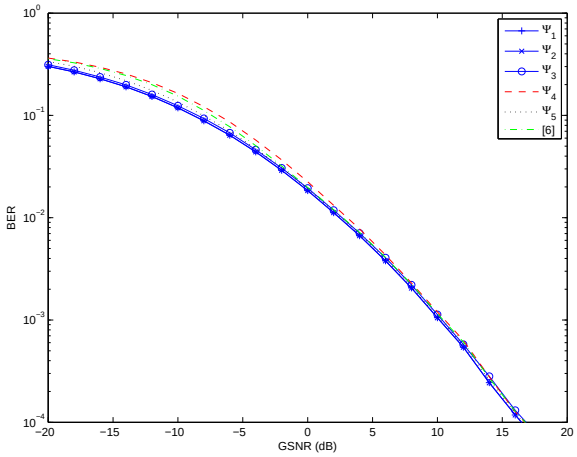

Fig. 8. BER vs. GSNR when $\gamma = 4$ and $\alpha = 0.5$.

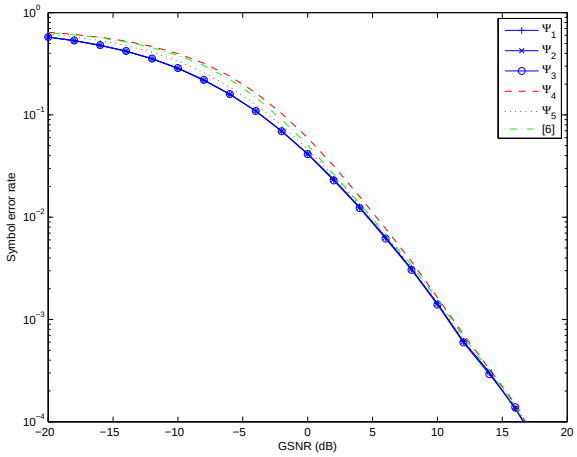

Fig. 9. Symbol error rate vs. GSNR when $\gamma = 1$ and $\alpha = 0.5$ for QPSK.

error MSE increases from 0.002 to 0.02, both of which are attainable using practical estimators designed in the literature. Fig. 8 shows the BER vs. GSNR when $\gamma = 4$ to examine the effect of varying γ, which is the case when one considers the system performance in different scenarios, for example, different densities of interferers [3, eq. (18)]. One sees from Fig. 8 that the new detectors still have the best performances, in all the cases considered. The performance gains of the new detectors do not change much compared with Fig. 2. Fig. 9 shows the symbol error rate vs. GSNR for quaternary phase shift keying (QPSK). Similar observations to those from Fig. 2 can be made. Moreoever, QPSK has poorer performance than BPSK in Fig. 2 under the same conditions.

Finally, the complexities of the detectors are compared as follows. For Ψ_1 using LS, Ψ_2 using LS and Ψ_3 using LS, PMM and MMM, closed-form expressions for their model parameters are available. Thus, their complexities in terms of model parameter calculation are comparable with those of the Myriad detector and the existing detector in [6] that also have closed-form expressions, although the new approximations do have more complicated functions, such as power and

exponential functions, in their closed-form expressions.

For Ψ_1 using PMM and Ψ_2 using PMM, their model parameters do not have any closed-form expressions. Instead, two-dimensional searches for Ψ_1 and one-dimensional searches for Ψ_2 are required. Using a desktop PC with i7 CPU and 8 GB memory and the tic-toc operations in MATLAB, a 11×11 two-dimensional search takes on average 2.8 seconds. From Tables I and II, the longest search is the two-dimensional search for b_1 and d_1 in Ψ_1 when $\alpha = 0.3$. In this case, using values from LS in Table I as starting points, 7 selective searches each of 21 grid points are required to find b_1 and 4 selective searches each of 21 grid points are required to find d_1, as b_1 has 7 digits and d_1 has 4 digits if the third digit after the decimal point is required. Thus, the total is about $28\times4\times2.8 = 313.6$ seconds, where 28 is the number of selective searches and 4 is the number of 11×11 two-dimensional grids in each search. Using the same hardware and software, the Myriad detector takes 1.6 seconds on average. These calculations include the time required to compute the decision variables and all necessary parameters. Thus, Ψ_1 takes about 196 times longer than the Myriad detector or consumes about 23 dB more power than the Myriad detector using PMM. However, these searches are on-off as long as the new detectors operate in a homogeneous environment. From Fig. 3, Ψ_1 has a performance gain of about 2 dB over the Myriad detector, when $\alpha = 0.3$. Thus, the power penalty incurred from the two-dimensional search may be completely compensated after 12 operations. From the 13th operation, Ψ_1 will provide gains over the Myriad detector. For other values of α and Ψ_2, the search will be quicker and less power-consuming too. The aforementioned figures are only indicative and rough estimates. A more accurate comparison will depend on the practical hardware as well as the actual operating environment.

On the other hand, if one does require closed-form expressions for Ψ_1 using PMM and Ψ_2 using PMM, one can simplify them. From (7), any use of (7c) or (7d) will lead to intractable solutions, due to the highly nonlinear functions of the p-th power in (7d) and the square root in (7c). Thus, to obtain closed-form expressions for Ψ_1 using PMM, one can use two closed-form expressions from LS to replace (7c) and (7d). This gives

$$a_1 = \frac{1 - \frac{\Gamma(1/\alpha)}{\sqrt{d_1}\alpha}}{\frac{\pi}{\sqrt{b_1}} - \frac{\pi}{\sqrt{d_1}}} \tag{31a}$$

$$c_1 = \frac{1 - \frac{\Gamma(1/\alpha)}{\sqrt{b_1}\alpha}}{\frac{\pi}{\sqrt{d_1}} - \frac{\pi}{\sqrt{b_1}}} \tag{31b}$$

where b_1 and d_1 are determined in closed-form by (5) when $\alpha > 1$ and (6) when $\alpha < 1$. Similarly, for Ψ_1 using PMM, one has

$$a_2 = \frac{1}{\pi\alpha}\Gamma(1/\alpha) \tag{32a}$$

$$\begin{aligned} b_2 &= \frac{d_2^{\frac{3}{4}}(\frac{c_2^2}{4d_2} - 1)^{\frac{1}{4}}}{\sqrt{2}\Gamma(3/2)B(1/2,3/2)P_{-1}^{-\frac{1}{2}}(\frac{c_2}{2\sqrt{d_2}})} \\ &- \frac{\sqrt{d_2}\Gamma(1/\alpha)}{\pi\alpha}\frac{P_0^{-\frac{1}{2}}(\frac{c_2}{\sqrt{d_2}})}{P_{-1}^{-\frac{1}{2}}(\frac{c_2}{\sqrt{d_2}})},\ c_2^2 \geq 4d_2 \end{aligned} \tag{32b}$$

$$\begin{aligned} b_2 &= \frac{d_2^{\frac{3}{4}}(1 - \frac{c_2^2}{4d_2})^{\frac{1}{4}}}{\sqrt{2}\Gamma(3/2)B(1/2,3/2)P_0^{-\frac{1}{2}}(\frac{c_2}{2\sqrt{d_2}})} \\ &- \frac{t\sqrt{d_2}\Gamma(1/\alpha)}{\pi\alpha}\frac{P_{-1}^{-\frac{1}{2}}(\frac{c_2}{\sqrt{d_2}})}{P_0^{-\frac{1}{2}}(\frac{c_2}{\sqrt{d_2}})},\ c_2^2 < 4d_2 \end{aligned} \tag{32c}$$

where c_2 and d_2 are given by (9). Essentially, this is a combination of LS and PMM to simplify PMM-based approximations.

V. Conclusion

New approximations to the PDF of the SαS distribution have been proposed. Numerical results have shown that the new approximations have high accuracy in most cases. Numerical results have also shown that detectors based on these new approximations outperform the existing detector in most cases, especially when the value of α is small. A future work includes the experimental verification of the proposed detectors in a wireless sensing system.

Appendix A
Derivations of (7)

In this appendix, the methods of calculating the parameters of $g_1(x)$ are derived. One has

$$f_\alpha(0) = \frac{1}{\pi}\int_0^\infty e^{-\omega^\alpha}d\omega = \frac{1}{\pi\alpha}\Gamma\left(\frac{1}{\alpha}\right) \tag{33}$$

where [12, eq. (3.478.1)] has been used. Using $f_\alpha(0) = g_1(0)$, one has (7a). Also,

$$1 = 2\int_0^\infty [\frac{a_1}{1+b_1x^2} + \frac{c_1}{1+d_1x^2}]dx. \tag{34}$$

The integrations in (34) can be solved using [12, eq. (3.252.2)] to give (7b). Also, from the Parseval's theorem, one has

$$\begin{aligned} \frac{2^{-1/\alpha}}{\pi\alpha}\Gamma\left(\frac{1}{\alpha}\right) &= \int_{-\infty}^\infty [\frac{a_1^2}{(1+b_1x^2)^2} \\ &+ \frac{c_1^2}{(1+d_1x^2)^2} + \frac{2a_1c_1}{(1+b_1x^2)(1+d_1x^2)}]dx. \end{aligned} \tag{35}$$

These integrations can be solved using [12, eq. (3.252.2)] and [12, eq. (3.264.2)] to give (7c). Finally, the p-th order moment of $g_1(x)$ is given by

$$\int_{-\infty}^\infty |x|^p g_1(x)dx = \int_{-\infty}^\infty |x|^p[\frac{a_1}{1+b_1x^2} + \frac{c_1}{1+d_1x^2}]dx. \tag{36}$$

The two integrations can directly be solved using [12, eq. (3.252.2)] to give (7d). The moments of $f_\alpha(x)$ are given by [11, eq. (6)]. By equating them, one has (7d).

APPENDIX B
DERIVATIONS OF (10) - (13)

First, using $f_\alpha(0) = g_2(0)$, one has

$$a_2 = \frac{1}{\pi\alpha}\Gamma\left(\frac{1}{\alpha}\right). \tag{37}$$

Second, one has

$$1 = 2\int_0^\infty \frac{a_2 + b_2x^2}{1 + c_2x^2 + d_2x^4}dx. \tag{38}$$

Using variable transformation as $t = \sqrt{d_2}x^2$, one further has

$$\begin{aligned} &2\int_0^\infty \frac{a_2 + b_2x^2}{1 + c_2x^2 + d_2x^4}dx \\ &= \frac{1}{d_2^{\frac{1}{4}}}[a_2\int_0^\infty \frac{1}{\sqrt{t}}\frac{1}{1 + \frac{c_2}{\sqrt{d_2}}t + t^2}dt \\ &+ \frac{b_2}{\sqrt{d_2}}\int_0^\infty \frac{t^{\frac{1}{2}}}{1 + \frac{c_2}{\sqrt{d_2}}t + t^2}dt]. \end{aligned} \tag{39}$$

The two integrals in (39) can be solved using [12, eq. (3.252.11)] and [12, eq. (3.252.10)] twice

$$\begin{aligned} &\frac{\sqrt{2}a_2}{d_2^{\frac{1}{4}}}\left(\frac{c_2^2}{4d_2} - 1\right)^{-\frac{1}{4}}\Gamma\left(\frac{3}{2}\right)B\left(\frac{3}{2},\frac{1}{2}\right)P_0^{-\frac{1}{2}}\left(\frac{c_2}{2\sqrt{d_2}}\right) \\ + &\frac{\sqrt{2}b_2}{d_2^{\frac{3}{4}}}\left(\frac{c_2^2}{4d_2} - 1\right)^{-\frac{1}{4}}\Gamma\left(\frac{3}{2}\right)B\left(\frac{1}{2},\frac{3}{2}\right)P_{-1}^{-\frac{1}{2}}\left(\frac{c_2}{2\sqrt{d_2}}\right) = 1 \end{aligned} \tag{40}$$

for $c_2^2 \geq 4d_2$ and for $c_2^2 < 4d_2$

$$\begin{aligned} &\frac{\sqrt{2}a_2\arccos\left(\frac{c_2}{2\sqrt{d_2}}\right)}{d_2^{\frac{1}{4}}\left(1 - \frac{c_2^2}{4d_2}\right)^{\frac{1}{4}}}\Gamma\left(\frac{3}{2}\right)B\left(\frac{1}{2},\frac{3}{2}\right)P_{-1}^{-\frac{1}{2}}\left(\frac{c_2}{2\sqrt{d_2}}\right) \\ + &\frac{\sqrt{2}b_2\arccos\left(\frac{c_2}{2\sqrt{d_2}}\right)}{d_2^{\frac{3}{4}}\left(1 - \frac{c_2^2}{4d_2}\right)^{\frac{1}{4}}}\Gamma\left(\frac{3}{2}\right)B\left(\frac{3}{2},\frac{1}{2}\right)P_0^{-\frac{1}{2}}\left(\frac{c_2}{2\sqrt{d_2}}\right) = 1 \end{aligned} \tag{41}$$

where $P(\cdot)$ is the associated Legendre function of the first kind [12, eq. (8.702.1)]. Also,

$$\begin{aligned} \frac{2^{-1/\alpha}}{\pi\alpha}\Gamma\left(\frac{1}{\alpha}\right) &= \int_{-\infty}^\infty g_2^2(x)dx \\ &= \frac{1}{d_2^{\frac{1}{4}}}\int_0^\infty \frac{(a_2 + \frac{b_2}{\sqrt{d_2}}t)^2}{\sqrt{t}(1 + \frac{c_2}{\sqrt{d_2}}t + t^2)^2}dt. \end{aligned} \tag{42}$$

This gives $\frac{1}{d_2^{\frac{1}{4}}}\int_0^\infty \frac{a_2^2}{\sqrt{t}(1+\frac{c_2}{\sqrt{d_2}}t+t^2)^2}dt + \frac{1}{d_2^{\frac{1}{4}}}\int_0^\infty \frac{\frac{2a_2b_2}{\sqrt{d_2}}t}{\sqrt{t}(1+\frac{c_2}{\sqrt{d_2}}t+t^2)^2}dt + \frac{1}{d_2^{\frac{1}{4}}}\int_0^\infty \frac{\frac{b_2^2}{d_2}t^2}{\sqrt{t}(1+\frac{c_2}{\sqrt{d_2}}t+t^2)^2}dt$, which can be solved by using [12, eq. (3.252.11)] and [12, eq. (3.252.10)] three times to give

$$\begin{aligned} &\frac{2^{-\frac{1}{\alpha}}}{\pi\alpha}\Gamma\left(\frac{1}{\alpha}\right) \\ &= \frac{2^{\frac{3}{2}}a_2^2}{d_2^{\frac{1}{4}}}\left(\frac{c_2^2}{4d_2} - 1\right)^{-\frac{3}{4}}\Gamma\left(\frac{5}{2}\right)B\left(\frac{7}{2},\frac{1}{2}\right)P_1^{-\frac{3}{2}}\left(\frac{c_2}{2\sqrt{d_2}}\right) \\ &+ \frac{2^{\frac{5}{2}}a_2b_2}{d_2^{\frac{3}{4}}}\left(\frac{c_2^2}{4d_2} - 1\right)^{-\frac{3}{4}}\Gamma\left(\frac{5}{2}\right)B\left(\frac{5}{2},\frac{3}{2}\right)P_0^{-\frac{3}{2}}\left(\frac{c_2}{2\sqrt{d_2}}\right) \\ &+ \frac{2^{\frac{3}{2}}b_2^2}{d_2^{\frac{5}{4}}}\left(\frac{c_2^2}{4d_2} - 1\right)^{-\frac{3}{4}}\Gamma\left(\frac{5}{2}\right)B\left(\frac{3}{2},\frac{5}{2}\right)P_{-1}^{-\frac{3}{2}}\left(\frac{c_2}{2\sqrt{d_2}}\right) \end{aligned} \tag{43}$$

and

$$\begin{aligned} &\frac{2^{-1/\alpha}}{\pi\alpha}\Gamma\left(\frac{1}{\alpha}\right) \\ &= \frac{2^{\frac{3}{2}}a_2^2\arccos\left(\frac{c_2}{2\sqrt{d_2}}\right)}{d_2^{\frac{1}{4}}\left(1 - \frac{c_2^2}{4d_2}\right)^{\frac{3}{4}}}\Gamma\left(\frac{5}{2}\right)B\left(\frac{1}{2},\frac{7}{2}\right)P_{-2}^{-\frac{3}{2}}\left(\frac{c_2}{2\sqrt{d_2}}\right) \\ &+ \frac{2^{\frac{5}{2}}a_2b_2\arccos\left(\frac{c_2}{2\sqrt{d_2}}\right)}{d_2^{\frac{3}{4}}\left(1 - \frac{c_2^2}{4d_2}\right)^{\frac{3}{4}}}\Gamma\left(\frac{5}{2}\right)B\left(\frac{3}{2},\frac{5}{2}\right)P_{-1}^{-\frac{3}{2}}\left(\frac{c_2}{2\sqrt{d_2}}\right) \\ &+ \frac{2^{\frac{3}{2}}b_2^2\arccos\left(\frac{c_2}{2\sqrt{d_2}}\right)}{d_2^{\frac{5}{4}}\left(1 - \frac{c_2^2}{4d_2}\right)^{\frac{3}{4}}}\Gamma\left(\frac{5}{2}\right)B\left(\frac{5}{2},\frac{3}{2}\right)P_0^{-\frac{3}{2}}\left(\frac{c_2}{2\sqrt{d_2}}\right) \end{aligned} \tag{44}$$

for $c_2^2 \geq 4d_2$ and $c_2^2 < 4d_2$, respectively. Also, for the moments of $g_2(x)$, one has $\int_{-\infty}^\infty \frac{(a_2+b_2x^2)|x|^p}{1+c_2x^2+d_2x^4}dx = \frac{1}{d_2^{\frac{p+1}{4}}}\int_0^\infty \frac{(a_2+\frac{b_2}{\sqrt{d_2}}t)t^{\frac{p-1}{2}}}{1+\frac{c_2}{\sqrt{d_2}}t+t^2}dt$, which can be expanded as $\frac{1}{d_2^{\frac{p+1}{4}}}\int_0^\infty \frac{a_2t^{\frac{p-1}{2}}}{1+\frac{c_2}{\sqrt{d_2}}t+t^2}dt + \frac{1}{d_2^{\frac{p+1}{4}}}\int_0^\infty \frac{\frac{b_2}{\sqrt{d_2}}t^{\frac{p+1}{2}}}{1+\frac{c_2}{\sqrt{d_2}}t+t^2}dt$, each solved using [12, eq. (3.252.11)] and [12, eq. (3.252.10)] to give

$$\begin{aligned} &\frac{2^{p+1}\Gamma\left(\frac{p+1}{2}\right)\Gamma\left(-\frac{p}{\alpha}\right)}{\alpha\sqrt{\pi}\Gamma\left(-\frac{p}{2}\right)} \\ &= \frac{\sqrt{2}a_2}{d_2^{\frac{p+1}{4}}\left(\frac{c_2^2}{4d_2} - 1\right)^{\frac{1}{4}}}\Gamma\left(\frac{3}{2}\right)B\left(\frac{3-p}{2},\frac{p+1}{2}\right)P_{-\frac{p}{2}}^{-\frac{1}{2}}\left(\frac{c_2}{2\sqrt{d_2}}\right) \\ &+ \frac{\sqrt{2}b_2}{d_2^{\frac{p+3}{4}}\left(\frac{c_2^2}{4d_2} - 1\right)^{\frac{1}{4}}}\Gamma\left(\frac{3}{2}\right)B\left(\frac{1-p}{2},\frac{p+3}{2}\right)P_{-\frac{p+1}{2}}^{-\frac{1}{2}}\left(\frac{c_2}{2\sqrt{d_2}}\right) \end{aligned} \tag{45}$$

and

$$\begin{aligned} \frac{2^{p+1}\Gamma\left(\frac{p+1}{2}\right)\Gamma\left(-\frac{p}{\alpha}\right)}{\alpha\sqrt{\pi}\Gamma\left(-\frac{p}{2}\right)} &= \frac{\sqrt{2}a_2\arccos\left(\frac{c_2}{2\sqrt{d_2}}\right)}{d_2^{\frac{p+1}{4}}\left(1 - \frac{c_2^2}{4d_2}\right)^{\frac{1}{4}}}\Gamma\left(\frac{3}{2}\right) \\ \cdot B\left(\frac{p+1}{2},\frac{3-p}{2}\right)P_{\frac{p-2}{2}}^{-\frac{1}{2}}\left(\frac{c_2}{2\sqrt{d_2}}\right) &+ \frac{\sqrt{2}b_2\arccos\left(\frac{c_2}{2\sqrt{d_2}}\right)}{d_2^{\frac{p+3}{4}}\left(1 - \frac{c_2^2}{4d_2}\right)^{\frac{1}{4}}} \\ \cdot\Gamma\left(\frac{3}{2}\right)B\left(\frac{p+3}{2},\frac{1-p}{2}\right)P_{\frac{p}{2}}^{-\frac{1}{2}}\left(\frac{c_2}{2\sqrt{d_2}}\right) & \end{aligned} \tag{46}$$

for $c_2^2 \geq 4d_2$ and $c_2^2 < 4d_2$, respectively.

Using (37) in (40), (43) and (45), one has three equations that are functions of d_2, $\frac{b_2}{\sqrt{d_2}}$ and $\frac{c_2}{2\sqrt{d_2}}$ only. Using these three equations to eliminate d_2, one can derive a second-order polynomial of $\frac{b_2}{\sqrt{d_2}}$ in (11), whose coefficients are functions of $\frac{c_2}{2\sqrt{d_2}}$ only as given by

$$u = 2^{\frac{3}{2}}\left(\frac{c_2^2}{4d_2}-1\right)^{-\frac{3}{4}}\Gamma\left(\frac{5}{2}\right)B\left(\frac{3}{2},\frac{5}{2}\right)P_{-1}^{-\frac{3}{2}}\left(\frac{c_2}{2\sqrt{d_2}}\right) \tag{47a}$$

$$\begin{aligned} v &= 2^{\frac{5}{2}}a_2\left(\frac{c_2^2}{4d_2}-1\right)^{-\frac{3}{4}}\Gamma\left(\frac{5}{2}\right)B\left(\frac{5}{2},\frac{3}{2}\right)P_{0}^{-\frac{3}{2}}\left(\frac{c_2}{2\sqrt{d_2}}\right) \\ &- \frac{2^{\frac{1}{2}-\frac{1}{\alpha}}\Gamma\left(\frac{1}{\alpha}\right)}{\pi\alpha\left(\frac{c_2^2}{4d_2}-1\right)^{\frac{1}{4}}}\Gamma\left(\frac{3}{2}\right)B\left(\frac{1}{2},\frac{3}{2}\right)P_{-1}^{-\frac{1}{2}}\left(\frac{c_2}{2\sqrt{d_2}}\right) \end{aligned} \tag{47b}$$

$$\begin{aligned} w &= a_2^2 2^{\frac{3}{2}}\left(\frac{c_2^2}{4d_2}-1\right)^{-\frac{3}{4}}\Gamma\left(\frac{5}{2}\right)B\left(\frac{7}{2},\frac{1}{2}\right)P_{1}^{-\frac{3}{2}}\left(\frac{c_2}{2\sqrt{d_2}}\right) \\ &- \frac{2^{\frac{1}{2}-\frac{1}{\alpha}}\Gamma\left(\frac{1}{\alpha}\right)}{\pi\alpha\left(\frac{c_2^2}{4d_2}-1\right)^{\frac{1}{4}}}\Gamma\left(\frac{3}{2}\right)B\left(\frac{1}{2},\frac{3}{2}\right)P_{0}^{-\frac{1}{2}}\left(\frac{c_2}{2\sqrt{d_2}}\right) \end{aligned} \tag{47c}$$

Solving this polynomial, one can express $\frac{b_2}{\sqrt{d_2}}$ as a function of $\frac{c_2}{2\sqrt{d_2}}$. Using this expression in (10), one has an equation for $\frac{c_2}{2\sqrt{d_2}}$ only. Similarly, one can derive (12) and (13), where the polynomial coefficients for $c_2^2 < 4d_2$ are

$$u' = 2^{\frac{3}{2}}\left(1-\frac{c_2^2}{4d_2}\right)^{-\frac{3}{4}}t\Gamma\left(\frac{5}{2}\right)B\left(\frac{5}{2},\frac{3}{2}\right)P_{0}^{-\frac{3}{2}}\left(\frac{c_2}{2\sqrt{d_2}}\right) \tag{48a}$$

$$\begin{aligned} v' &= 2^{\frac{5}{2}}a_2\left(1-\frac{c_2^2}{4d_2}\right)^{-\frac{3}{4}}t\Gamma\left(\frac{5}{2}\right)B\left(\frac{3}{2},\frac{5}{2}\right)P_{-1}^{-\frac{3}{2}}\left(\frac{c_2}{2\sqrt{d_2}}\right) \\ &- \frac{2^{\frac{1}{2}-\frac{1}{\alpha}}\Gamma\left(\frac{1}{\alpha}\right)}{\pi\alpha\left(1-\frac{c_2^2}{4d_2}\right)^{\frac{1}{4}}}t\Gamma\left(\frac{3}{2}\right)B\left(\frac{3}{2},\frac{1}{2}\right)P_{0}^{-\frac{1}{2}}\left(\frac{c_2}{2\sqrt{d_2}}\right) \end{aligned} \tag{48b}$$

$$\begin{aligned} w' &= a_2^2 2^{\frac{3}{2}}\left(1-\frac{c_2^2}{4d_2}\right)^{-\frac{3}{4}}t\Gamma\left(\frac{5}{2}\right)B\left(\frac{1}{2},\frac{7}{2}\right)P_{-2}^{-\frac{3}{2}}\left(\frac{c_2}{2\sqrt{d_2}}\right) \\ &- \frac{2^{\frac{1}{2}-\frac{1}{\alpha}}\Gamma\left(\frac{1}{\alpha}\right)}{\pi\alpha\left(1-\frac{c_2^2}{4d_2}\right)^{\frac{1}{4}}}t\Gamma\left(\frac{3}{2}\right)B\left(\frac{3}{2},\frac{1}{2}\right)P_{-1}^{-\frac{1}{2}}\left(\frac{c_2}{2\sqrt{d_2}}\right). \end{aligned} \tag{48c}$$

APPENDIX C
DERIVATIONS OF (16) - (24)

The first equation (16a) comes directly from $f_\alpha(0) = g_3(0)$. Also,

$$1 = \frac{2a_3}{b_3^{\frac{1}{\alpha+1}}}\int_0^\infty \frac{1}{1+t^{\alpha+1}}dt. \tag{49}$$

The last integral can be solved using [12, eq. (3.241.2)] to give (16b). Similarly, one has

$$\frac{2^{-1/\alpha}}{\pi\alpha}\Gamma(\frac{1}{\alpha}) = \int_{-\infty}^{\infty} g_3^2(x)dx = \frac{2a_3^2}{b_3^{\frac{1}{\alpha+1}}}\int_0^\infty \frac{1}{(1+t^{\alpha+1})^2}dt. \tag{50}$$

Using [12, eq. (3.241.5)], one has (16c). Also, one has [9]

$$\lim_{x\to\infty} f_\alpha(x) = \frac{\alpha\Gamma(\alpha)\sin(\frac{\alpha\pi}{2})}{\pi x^{\alpha+1}}. \tag{51}$$

Since $\lim_{x\to\infty} g_3(x) = \frac{a_3}{b_3 x^{\alpha+1}}$, one has (16d). Also, the p-th order moment of $g_3(x)$ is derived as

$$\int_{-\infty}^{\infty}\frac{a_3|x|^p}{1+b_3|x|^{\alpha+1}}dx = \frac{2a_3}{b_3^{\frac{p+1}{\alpha+1}}}\int_0^\infty \frac{t^p}{1+t^{\alpha+1}}dt. \tag{52}$$

The last integral can be solved using [12, eq. (3.241.2)] to give (23).

REFERENCES

[1] E.J. Wegman, S.G. Schwartz, and J.B. Thomas (eds.), *Topics in Non-Gaussian Signal Processing*. New York: Academic Press, 1989.

[2] B. Mandelbrot, "The variation of some other speculative prices," *Journal of Business*, vol. 40, pp. 393-413, Oct. 1967.

[3] J. Ilow and D. Hatzinakos, "Analytic alpha-stable noise modeling in a field of Poisson interferers and scatters," *IEEE Trans. Signal Processing*, vol. 46, pp. 1601-1611, June 1998.

[4] G. Samorodnitsky and M.S. Taqqu, *Stable Non-Gaussian Random Processes: Stochastic Models With Infinite Variance*. New-York: Chapman & Hall, 1994.

[5] J.P. Nolan, "Numerical calculation of stable densities and distribution functions," *Communications in Statistics. Stochastic Models*, vol. 13, pp. 759-774, 1997.

[6] J.H. Mcculloch, "Numerical approximation of the symmetric stable distribution and density", in the book "A practical guide to heavy tails: statistical techniques and applications", Birkhauser: Boston, MA, 1998.

[7] A. Swami, "Non-Gaussian mixture models for detection and estimation in heavy-tailed noise," *Proc. ICASSP'00*, pp. 3802-3805, 2000.

[8] E.E. Kuruoğlu, C. Molina, and W.J. Fitzgerald, "Approximation of α-stable probability densitities using finite mixtures of Gaussians," in *Proc. EUSIPCO'98*, Rhodes, Greece, Sept. 11, 1998.

[9] G.A. Tsihrintzis and C.L. Nikias, "Performance of optimum and suboptimum receivers in the presence of impulsive noise modeled as an alpha-stable process," *IEEE Trans. Commun.*, vol. 43, no. 2/3/4, pp. 904-914, Feb./Mar./Apr. 1995.

[10] C.L. Nikias and M. Shao, *Signal Processing with Alpha-Stable Distributions and Applications*. New York: Chapman-Hall, 1996.

[11] X. Ma and C.L. Nikias, "Parameter estimation and blind channel identification in impulsive signal environments," *IEEE Trans. Signal Processing*, vol. 43, Dec. 1995.

[12] I.S. Gradshteyn and I.M. Ryzhik, *Table of Integrals, Series, and Products*, 6th Ed., Academic Press: London, 2000.

[13] J.G. Gonzalez and G.R. Arce, "Optimality of the myriad filter in practical impulsive-noise environments," *IEEE Trans. Sig. Processing*, vol. 49, pp. 438 - 441, Feb. 2001.

[14] J.G. Gonzalez and G.R. Arce, "Statistically-efficient filtering in impulsive environments: weighted myriad filters," *EURASIP J. Applied Signal Processing*, vol. 2002, pp. 4-20, Jan. 2002.

[15] C.L. Brown and A.M. Zoubir, "A nonparametric approach to signal detection in impulsive interference," *IEEE Trans. Signal Process.*, vol. 48, no. 9, pp. 2665-2669, Sept. 2000.

[16] S. Zozor, J. Brossier, and P. Amblard, "A parametric approach to suboptimal signal detection in $alpha$-stable noise," *IEEE Trans. Sigal Process.*, vol. 54, no. 12, pp. 4497-4509, Dec. 2006.

[17] G. Gonzalez, "Robust techniques for wireless communications in non-Gaussian environments," Ph.D. Dissertation, University of Delaware, Newark, DE, USA, 1997.

[18] I.A. Koutrouvelis, "Regression-type estimation of the parameters of stable laws," *J. Amer. Statist. Assoc.*, vol. 75, pp 918-928, Dec. 1980.

[19] S. Arnon, J.R. Barry, G.K. Karagiannidis, R. Schober and M. Uysal, *Advanced Optical Wireless Communication Systems*, Cambridge University Press: Cambridge, UK. 2012.

[20] C. Buratti, M. Martalo, R. Verdone, G. Ferrari, *Sensor Networks with IEEE 802.15.4 Systems: Distributed Processing, MAC and Connectivity*, Springer: London, UK. 2011.

[21] J.D. Taylor (ed.), *Introduction to Ultra-Wideband Radar Systems*, CRC Press: FL, USA. 1995.

[22] R. van Langevelde, M. van Elzakker, D. van Goor, H Termeer, J. Moss, A.J. Davie, "An ultra-low-power 868/915 MHz RF transceiver for wireless sensor network applications," *Proc. RFIC 2009*, pp. 113 - 116, Boston, USA, June 2009.
[23] C. Cordeiro, M. Ghosh, D. Cavacanti, K. Challapali, "Spectrum sensing for dynamic spectrum access of TV bands," *Proc. CrownCom 2007*, pp. 225 - 233, Orlando, USA, Aug. 2007.
[24] Z. Quan, W. Zhang, S.J. Shellhammer, A.H. Sayed, "Optimal spectral feature detection for spectrum sensing at very low SNR," *IEEE Trans. Commun.*, vol. 59, pp. 201 - 212, Jan. 2011.
[25] T.S. Rappaport, *Wireless Communications: Principles and Practice*, 2nd Ed. New York: Prentice Hall, 2002.